

**Compensation effect and differential capacitance analysis of electronic energy band structure in relaxed InAs quantum dots**

J. F. Chen, Ross C. C. Chen, C. H. Chiang, M. C. Hsieh, Y. C. Chang, and Y. F. Chen

Citation: [Journal of Applied Physics](#) **108**, 063705 (2010); doi: 10.1063/1.3467938

View online: <http://dx.doi.org/10.1063/1.3467938>

View Table of Contents: <http://scitation.aip.org/content/aip/journal/jap/108/6?ver=pdfcov>

Published by the [AIP Publishing](#)

---

**Articles you may be interested in**

[Electronic structure of self-assembled InGaAs/GaAs quantum rings studied by capacitance-voltage spectroscopy](#)  
Appl. Phys. Lett. **96**, 033111 (2010); 10.1063/1.3293445

[Electron emission properties of relaxation-induced traps in InAs/GaAs quantum dots and the effect of electronic band structure](#)  
J. Appl. Phys. **102**, 043705 (2007); 10.1063/1.2770817

[Effect of incorporating an InAlAs layer on electron emission in self-assembled InAs quantum dots](#)  
J. Appl. Phys. **99**, 014303 (2006); 10.1063/1.2150258

[N incorporation into InGaAs cap layer in InAs self-assembled quantum dots](#)  
J. Appl. Phys. **98**, 113525 (2005); 10.1063/1.2140891

[Spin splitting of the electron ground states of InAs quantum dots](#)  
Appl. Phys. Lett. **80**, 4229 (2002); 10.1063/1.1483112

---



## Re-register for Table of Content Alerts

Create a profile.



Sign up today!



# Compensation effect and differential capacitance analysis of electronic energy band structure in relaxed InAs quantum dots

J. F. Chen,<sup>a)</sup> Ross C. C. Chen, C. H. Chiang, M. C. Hsieh, Y. C. Chang, and Y. F. Chen  
*Department of Electrophysics, National Chiao Tung University, Hsinchu, Taiwan 30050, Republic of China*

(Received 25 March 2010; accepted 29 June 2010; published online 17 September 2010)

The use of a differential capacitance technique for analyzing the effect of strain relaxation on the electronic energy band structure in relaxed InAs self-assembled quantum dots (QDs) is presented. Strain relaxation is shown to induce a deep defect state and compensate the ionized impurity in the bottom GaAs layer, leading to a double depletion width and a long emission time. An expression of capacitance at different frequency and voltage is derived for analyzing the experimental data. It has been shown that the relationship between the low-frequency and high-frequency capacitances can be well explained by a Schottky depletion model with a compensated concentration in the bottom GaAs layer. A simple expression is presented to account for the modulation of the free electrons in the top GaAs layer. This capacitance analysis shows a long low-energy tail for the electron ground state, suggesting not very uniform strain relaxation. The results of this study illustrate a carrier compensation effect of the defect state on the electronic energy band structure near the QDs. © 2010 American Institute of Physics. [doi:10.1063/1.3467938]

## I. INTRODUCTION

Understanding the energy band structure in InAs self-assembled quantum dots (QDs) (Refs. 1–15) is important for designing the QD devices such as photodetectors<sup>13,14</sup> or memory devices. In self-assembled InAs QDs, strong strain is built up in the QDs and neighboring GaAs layers. Previous experiments have shown pronounced tunneling emission for the electrons in the QDs escaping to the GaAs.<sup>9–11,16,17</sup> The built-up strain is expected to have a strong effect on the energy band structure and emission mechanism of the QDs. Recently, a significantly elongated electron emission time was observed in strain relaxed QDs.<sup>18</sup> Strain relaxation in the QDs can lead to the generation of threading dislocations in the top GaAs layer and lattice misfits near the QDs.<sup>19</sup> Capping the QDs with an InGaAs strain-relieving layer, strain relaxation in the QDs can be accommodated by the lattice misfits near the QDs and the top GaAs layer is dislocation-free.<sup>18</sup> Most of the lattice misfits were observed in the bottom GaAs layer under the QDs by transmission electron microscopy,<sup>18</sup> suggesting strain relaxation through the bottom GaAs layer. A relaxation-induced defect state at 0.37 eV has been observed in the bottom GaAs layer.<sup>19</sup> Understanding the energy band structure in the relaxed QDs is believed to shed light on the strain effect in the coherently strained QDs. Thus, in this paper, we have derived an expression of capacitance at different frequency and voltage to analyze the electronic band structure in the relaxed QDs. We found that the relaxation-induced defect state can compensate the background ionized impurity in the bottom GaAs layer, leading to a long emission time. Furthermore, strain relaxation induces a long low-energy tail for the electron ground state (EGS) of the QDs, consistent with optical spectra. We showed that the energy band structure near the QDs

can be well described by a Schottky depletion mode with a compensated background concentration in the bottom GaAs layer.

## II. THEORY

### A. Theory of capacitance-voltage (C-V) spectra

Based on experimental results, Fig. 1 shows a simplified electron energy band diagram where Fermi level is intersecting with a QD state for a carrier modulation. A relaxation-induced defect state at an energy below the QDs in the GaAs bottom layer is shown. This defect state can trap electrons and compensate the background concentration in the GaAs bottom layer from ionized impurity  $N_D$  to a compensated background concentration  $N'_D = N_D - N_t$ , assuming a uniform  $N_t$  in the bottom GaAs layer for simplicity. This compensa-

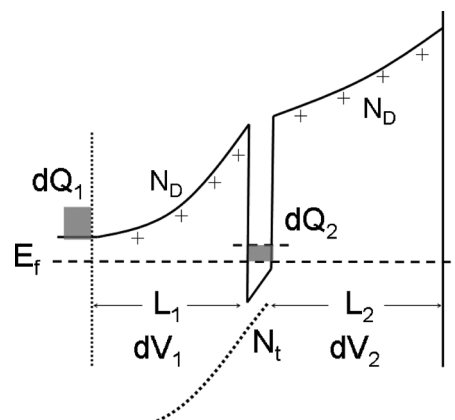


FIG. 1. Simplified electronic energy band diagram for a Schottky diode containing a QD layer for illustrating the modulation of the carriers  $dQ_1$  at the edge of the depletion region and the carriers  $dQ_2$  in the QDs at a confinement energy  $E$ . A relaxation-induced defect state  $N_t$  is shown in the GaAs bottom layer.

<sup>a)</sup>Electronic mail: jfchen@cc.nctu.edu.tw.

tion can effectively broaden the depletion region in the bottom GaAs layer near the QDs and suppress the tunneling emission. Applying a small change in the reverse voltage  $dV$  can modulate the carriers (per unit area)  $dQ_1$  at the edge of the depletion region and the carriers (per unit area)  $dQ_2$  in the QDs at a confinement energy  $E$ . From Gauss's law,  $dV$  can be expressed by the sum of the voltage changes across the two regions with their respective widths  $L_1$  and  $L_2$  as follows:

$$dV = dV_1 + dV_2 = \left( \frac{dQ_1}{\epsilon} \right) L_1 + \left( \frac{dQ_1 + dQ_2}{\epsilon} \right) L_2,$$

where  $\epsilon$  is the permittivity of the semiconductor. In a similar way as derived previously,<sup>20</sup>  $dQ_1 = \epsilon dV_1 / L_1$  is substituted into the above expression to obtain the ratio of the bias change across  $L_1$  to the total bias change as expressed by

$$\frac{dV_1}{dV} = \frac{L_1}{(L_1 + L_2) + \frac{dQ_2 L_1 L_2}{dV_1 \epsilon}}.$$

This bias ratio is related to the occupied density of states of the QDs,  $dQ_2/dV_1 \equiv C_Q$ . This density of states is related to capacitance as expressed by

$$C_L = \frac{dQ_1 + dQ_2}{dV} = \frac{dQ_1}{dV} + \frac{dQ_2}{dV} = \frac{dV_1 \epsilon}{dV L_1} + \frac{dQ_2 dV_1}{dV_1 dV} \\ = \frac{(C_1 + C_Q)C_2}{(C_1 + C_Q) + C_2},$$

where  $C_1 = \epsilon/L_1$  and  $C_2 = \epsilon/L_2$  are the geometric capacitance per unit area across  $L_1$  and  $L_2$ . This equation states that the capacitance is a parallel combination of  $C_1$  and  $C_Q$  followed by a series combination with  $C_2$ . This shall be the low-frequency capacitance  $C_L$  if the QD electrons can follow the frequency to be modulated. Under a high frequency where the QD electrons cannot be modulated,  $C_Q = 0$  and the capacitance is reduced to  $C_H = C_1 C_2 / (C_1 + C_2) = \epsilon / (L_1 + L_2)$ . Thus, the high-frequency capacitance can be used to obtain  $L_1$  ( $L_2$  is the designated spatial position the QDs). Substituting  $L_1$  into a Schottky depletion model yields the confinement energy  $E$  of the probed QD electrons as

$$E = V_1 + \phi_n = (q/2\epsilon)N_D' L_1^2 + (kT/q) \ln(N_C/N_D), \quad (1)$$

here  $N_D'$  is the compensated concentration in the bottom GaAs layer and  $N_C$  is the effective density of states in the GaAs conduction band (CB). The applied reverse voltage  $V_R$  is related to  $L_1$  by the voltage drop expression:  $V_R = V_1 + V_2 - V_{bi}$ , where

$$V_1 = (q/2\epsilon)N_D' L_1^2 \quad \text{and} \quad V_2 = (q/\epsilon)N_D' L_1 L_2 \\ + (q/2\epsilon)N_D L_2^2 - (L_2/\epsilon A) \int_{-\infty}^E C_Q dE, \quad (2)$$

here  $V_{bi} (= 0.8 \text{ eV})$  is the Schottky barrier height of the GaAs and  $A = 5 \times 10^{-3} \text{ cm}^2$  is the area of the diode studied here. The last term in  $V_2$  is the voltage drop due to the occupied electrons in the QDs below Fermi level. For simplicity, we have neglected the Fermi-Dirac distribution.

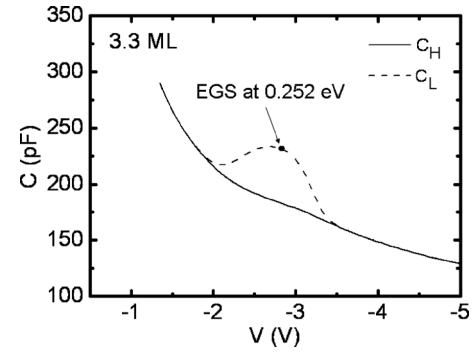


FIG. 2. Simulated low-frequency and high-frequency  $C$ - $V$  spectra for a Gaussian carrier distribution  $C_Q(E)$  at a depth of  $0.2 \mu\text{m}$  at  $E=0.252 \text{ eV}$  with a broadness of  $70 \text{ meV}$ . The low-frequency spectra display a  $C$  protrusion peaked at  $-2.8 \text{ V}$ .

Figure 2 shows simulated  $C$ - $V$  spectra for a Gaussian carrier distribution  $C_Q(E)$  to represent an electron state in the QD with a peak of  $680 \text{ pF}$  ( $=8.6 \times 10^{11}/\text{cm}^2 \text{ eV}$ ) at  $E = 0.252 \text{ eV}$  with a broadness of  $70 \text{ meV}$ . This carrier distribution  $C_Q(E)$  gives a total carrier density of  $7.9 \times 10^{10} \text{ cm}^{-2}$ , which is close to double the QD density corresponding to a capture of two electrons for an EGS. The simulation uses  $N_D = 1 \times 10^{17} \text{ cm}^{-3}$  and  $N_D' = N_D - N_i = 2.9 \times 10^{16} \text{ cm}^{-3}$  based on the experimental data to be shown. The simulated  $C_L$  displays a protrusion from  $-2$  to  $-3.5 \text{ V}$  with a peak at  $-2.8 \text{ V}$ , corresponding to the modulation of the peak of  $C_Q(E)$  at  $E=0.252 \text{ eV}$ .

We would like to emphasize that the above derivation works for large amplitude of reverse voltage so that the top GaAs layer is totally depleted of free electrons. For small amplitude of reverse voltage, Fermi level also modulates the free electrons in the top GaAs layer and introduce additional capacitance  $C_{\text{GaAs}} = dQ_{\text{GaAs}}/dV_1$ , where  $Q_{\text{GaAs}}$  is the modulated electron density in the top GaAs layer and shall be approximately proportional to the free carrier concentration at the GaAs CB near the QDs,  $n_o = N_C \exp(-V_1/kT)$  here  $V_1 = (q/2\epsilon)N_D' L_1^2$ . Decreasing reverse voltage will increase  $V_1$  to deplete  $Q_{\text{GaAs}}$  by  $Q_{\text{GaAs}} = Q_{\text{GaAs},o} \exp(-V_1/kT)$ . Accordingly, this additional capacitance rapidly decreases with increasing  $V_1$  by  $C_{\text{GaAs}} = dQ_{\text{GaAs}}/dV_1 = (1/kT)Q_{\text{GaAs}} = C_{\text{GaAs},o} \exp(-V_1/kT)$ . This effect is appreciable only when  $V_1(L_1)$  is very small. Under this condition, the modulated free carriers are nearly at the same spatial location as the QDs, leading to the low-frequency capacitance can be approximately expressed by  $C_L \cong C_2 + C_Q + C_{\text{GaAs}}$  while  $C_H \cong C_2$ . Thus, the effect of the carrier modulating in the top GaAs layer can be simply removed by subtracting  $C_{\text{GaAs}} = C_{\text{GaAs},o} \exp(-V_1/kT)$  from  $C_L$ . This effect, if not removed, would lead to an overestimation of the carrier density in the shallow QD electrons. This free carrier modulation effect is significant in the relaxed QDs because of the broad carrier depletion near the QDs.

### III. MEASUREMENT AND RESULTS

The InAs QD samples were grown by solid source molecular beam epitaxy in a Riber machine. On top of a  $n^+$ -GaAs(100) substrate, a  $0.3 \mu\text{m}$ -thick Si-doped GaAs ( $n = 1 \times 10^{18} \text{ cm}^{-3}$ ) was grown.

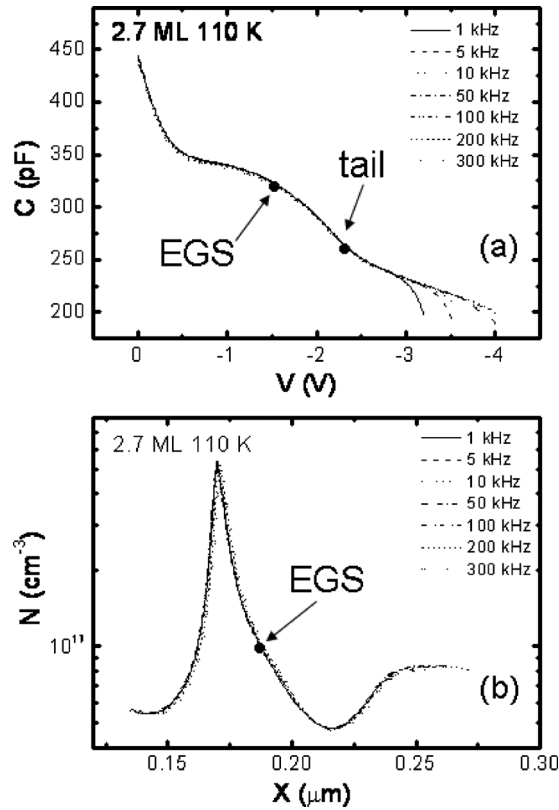


FIG. 3. (a) 110 K  $C$ - $V$  and (b) the converted carrier distribution for a nonrelaxed QD diode with InAs deposition thickness of 2.7 ML, illustrating a  $C$  plateau from  $-0.5$  to  $-2.5$  V related to the modulation of the QD electrons.

$\sim 1 \times 10^{17} \text{ cm}^{-3}$ ) barrier layer, an InAs layer with different deposition thickness from 2 to 3.3 monolayer (ML) was deposited at  $490^\circ \text{C}$  (at a rate of  $0.26 \text{ \AA/s}$ ) to form the QDs. Following the growth of the QDs layer, a  $60 \text{ \AA}$   $\text{In}_{0.15}\text{Ga}_{0.85}\text{As}$  strain-relieving capping layer and a  $0.2 \text{ }\mu\text{m}$ -thick Si-doped GaAs ( $\sim 10^{17} \text{ cm}^{-3}$ ) barrier layer were grown to terminate the growth. Relaxation in the QDs was achieved by increasing the InAs deposition thickness slightly beyond a critical thickness about 3 ML. A photoluminescence (PL) blueshift<sup>21</sup> about 80 meV is observed when strain relaxation in the QDs occurs. The QD sheet density is estimated to be  $\sim 3 \times 10^{10} \text{ cm}^{-2}$  from performing atomic force microscopy on sample surface where a layer of similar QDs was purposely grown. For  $C$ - $V$  profiling, Schottky diodes were realized by evaporating Al on sample surface with an area  $5 \times 10^{-3} \text{ cm}^2$ . A HP 4194A impedance analyzer was used for  $C$ - $V$  measurements with an oscillation level set at 50 mV.

## A. $C$ - $V$ - $F$ spectra

### 1. Coherently strained QDs

Figures 3(a) and 3(b) shows the 110 K  $C$ - $V$  and its converted carrier distribution using:  $N(w) = (C^3 / q\epsilon\epsilon_0(dC/dV))$  for a nonrelaxed QD diode with InAs deposition thickness of 2.7 ML. A  $C$  plateau from  $-0.5$  to  $-2.5$  V, corresponding to the modulation of the QD electrons, is visible. This plateau can be dissolved into a peak and a shoulder in the carrier distribution plot. The peak is attributed to the QD first excited state and the shoulder to the EGS of the QDs. When

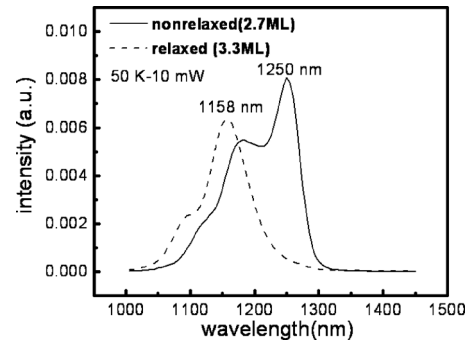


FIG. 4. 50 K PL spectra for nonrelaxed QDs with InAs deposition thickness of 2.7 ML and relaxed QDs with InAs deposition thickness of 3.3 ML. Strain relaxation causes a blueshift in the ground emission and produces a long low-energy tail.

temperature is lowered to 90 K, the shoulder displays frequency dispersion with an activation energy about 60 meV, suggesting a tunneling emission through the first excited state.<sup>18</sup> The emission energy of the first-excited state cannot be obtained from the  $C$ - $V$  spectra because no frequency dispersion is observed (the emission time is very short). We can estimate the confinement energy for the tail of the EGS because, at this nearly ending of modulation, the low-frequency capacitance shall approach the high-frequency capacitance. Let us choose  $C = 245 \text{ pF}$  at  $-2.5 \text{ V}$  as the tail of the QDs. This  $C$  gives  $L_1 + L_2 = 0.234 \text{ }\mu\text{m}$  ( $L_2 = 0.16 \text{ }\mu\text{m}$  is the designed QDs position from the surface). Substituting  $L_1 = 0.074 \text{ }\mu\text{m}$  and a  $N_D = 8 \times 10^{16} \text{ cm}^{-3}$  for  $N_D^+$  (seen in the carrier distribution) into Eq. (1) yields  $E = 0.320 \text{ eV}$  (at 110 K). As shown in Fig. 4, the 50 K PL spectra of this sample show a ground emission at 1250 nm (0.992 eV) with a narrow full width at half maximum of 35 meV. If we take this broadness as the broadness of the EGS, the EGS shall be at 0.303 eV. This gives the confinement energy of the hole ground state (HGS) of  $1.50 - 0.992 - 0.303 = 0.205 \text{ eV}$ , giving rise to a ratio of the confinement energy of EGS to HGS of 0.60 to 0.40, a value close to a previously reported 0.61:0.39.<sup>22</sup> The confinement energy of the EGS in the relaxed QDs shall be slightly smaller than that (0.303 eV) of the nonrelaxed QDs because the PL spectra show a blueshift of 79 meV when the relaxation occurs.<sup>21</sup> Figure 4 shows the PL ground emission at 1.071 eV for the relaxed QDs. This blueshift could move the EGS to 0.256 eV in the relaxed QDs assuming the above ratio of 0.6:0.4. This rough estimation shows that the EGS of the relaxed QDs shall be around 0.256 eV.

### 2. Relaxed QDs

Figures 5(a) and 5(b) show the 110 K  $C$ - $V$  and the converted carrier distribution for a relaxed QD diode with InAs deposition thickness of 3.3 ML. Its 50 K PL spectra are shown in Fig. 4. The  $C$ - $V$  spectra display two  $C$  plateaus. The plateau from  $-1.5$  to  $-3.4 \text{ V}$  is attributed to the QD electrons since its converted carrier profiling displays a similar feature as observed in the nonrelaxed QDs as follows: a peak at  $0.217 \text{ }\mu\text{m}$  from the first excited state (the QD spatial position is designed at  $0.2 \text{ }\mu\text{m}$ ), and a shoulder at  $0.225 \text{ }\mu\text{m}$  from the EGS. In contrast to no frequency dispersion observed in the nonrelaxed QDs, the  $C$ - $V$  spectra of the relaxed



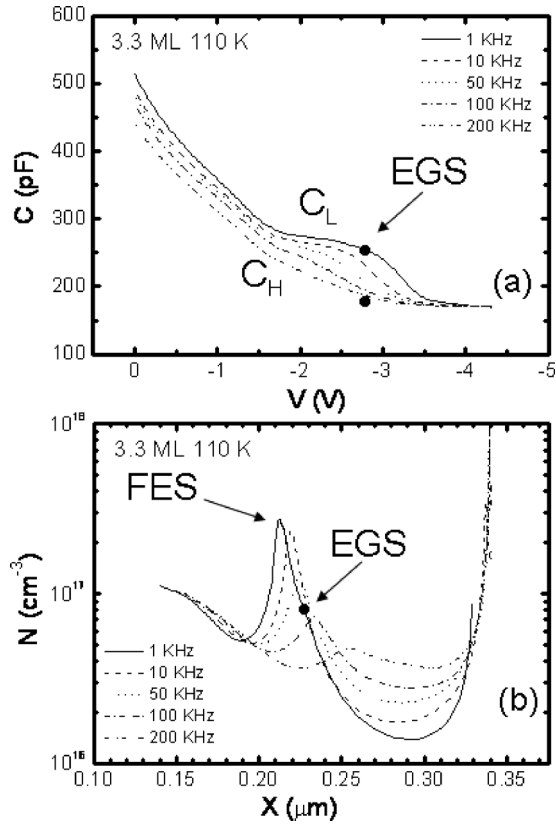


FIG. 5. (a) 110 K  $C$ - $V$  and (b) the converted electron distribution for a relaxed QD diode with InAs deposition thickness of 3.3 ML. The  $C$  plateau from  $-1.5$  to  $-3.4$  V is related to the modulation of the QD electrons and the  $C$  plateau starting from  $-3.5$  V is related to the relaxation-induced defect state.

QDs display frequency dispersion, suggesting a longer emission time. As shown in Fig. 5(a), the  $C$  protrusion diminishes with increasing frequency, reflective of an incapability of carrier modulation. Note that we observed no appreciable change in the  $C$ - $V$  spectra when frequency is lower than 1 kHz or higher than 200 kHz, and thus we take  $C$  at 1 kHz as  $C_L$  and at 200 kHz as  $C_H$  for the following analysis. The  $0.217 \mu\text{m}$  (at  $-2.54$  V) for the first excited state and the  $0.225 \mu\text{m}$  (at  $-2.8$  V) for the EGS cannot be interpreted as the positions of the edge of the depletion region because the concentration profiling in Fig. 5(b) is converted from the low-frequency capacitance which is affected by the modulation of the QDs. We should use the high-frequency capacitance. Figure 5(a) shows  $C_H=196$  pF at  $-2.54$  V (186 pF at  $-2.8$  V), which gives  $L_1+L_2=0.293 \mu\text{m}$  ( $0.308 \mu\text{m}$ ). After substituting from  $L_2=0.2 \mu\text{m}$  (the QDs position from the surface), we obtain  $L_1=0.093 \mu\text{m}$  ( $0.108 \mu\text{m}$ ). Substituting these  $L_1$  and  $N_D'=2.9 \times 10^{16} \text{ cm}^{-3}$  (to be determined in a later section) into Eq. (1) yield confinement energies of  $E=0.189$  eV and  $0.252$  eV for the first-excited state and EGS, respectively. The energy for the EGS is consistent with the one ( $0.256$  eV) estimated from the nonrelaxed QDs. Note that, during the simulation (in Fig. 2), an electron state at  $0.252$  eV would result in a  $C$  plateau peaked at  $-2.8$  V.

As shown in Fig. 5(a), the QD plateau is immediately followed by another  $C$  plateau (starting at  $-3.5$  V) which shows no frequency dispersion, suggesting an emission time

too long to be modulated. This plateau is attributed to the relaxation-induced defect state previously identified at  $0.37$  eV below the GaAs CB by deep-level transient spectroscopy.<sup>19</sup> The nearly voltage-independent capacitance suggests a pinning of Fermi level, implying a density of states being comparable to the background ionized impurity. Figure 5(b) shows drastic carrier depletion after the QD, suggesting a lower background concentration due to the carrier compensation of this defect state. Further decreasing reverse voltage will push down Fermi level to intersect with the defect state, giving rise to the second plateau at  $-3.5$  V (and the converted carrier peak) until all the trapped electrons are swept out of the defect state. This defect state behaves like a point defect state whose properties were previously studied in details.<sup>19</sup> It is similar as the one ( $0.395$  eV,  $\sigma=1 \times 10^{-16} \text{ cm}^2$ ) observed by Uchida *et al.*<sup>23</sup> in strain relaxed InGaAs/GaAs quantum well structures. The fact that the tail of the QD (at  $-3.4$  V) is immediately followed by the defect state stipulates that the tail of the EGS shall have a confinement energy of  $\sim 0.37$  eV.

## B. Compensation of background concentration

One pronounced feature associated with the defect state is the asymmetric carrier distribution on the sides of the QDs, as shown in Fig. 5(b). The top GaAs layer displays a normal carrier depletion near the QDs and a designated background concentration of  $N_D=1 \times 10^{17} \text{ cm}^{-3}$ . On the other hand, the bottom GaAs layer displays a lower background concentration with a nearly double depletion width, suggesting a compensation of the ionized impurity by the defect state. Based on a simple Schottky depletion model  $V=(q/2\epsilon)N_D L^2$ , a double depletion width would require a reduction in the background concentration from  $1 \times 10^{17}$  to  $2.5 \times 10^{16} \text{ cm}^{-3}$ , leading to an effective trapped concentration  $N_t=7.5 \times 10^{16} \text{ cm}^{-3}$ .

We can obtain a more accurate compensated concentration  $N_D'$  by using the voltage drop relationship:  $V_R=V_1+V_2-V_{bi}$  in Eq. (2). At  $-3.4$  V, the QDs are nearly empty of carriers and thus the term  $(L_2/\epsilon A)\int_{-\infty}^E C_Q dE$  in Eq. (2) can be neglected. Figure 5(a) shows  $C_H=173$  pF at  $-3.4$  V, corresponding to  $L_1=0.132 \mu\text{m}$ . Substituting the  $L_1$ ,  $L_2=0.2 \mu\text{m}$ ,  $V_R=3.4$  V and  $V_{bi}=0.8$  V into Eq. (2) gives  $N_D'=2.9 \times 10^{16} \text{ cm}^{-3}$ . This is close to the value ( $2.5 \times 10^{16} \text{ cm}^{-3}$ ) estimated from a double depletion width in the bottom GaAs layer. Substituting this  $N_D'$  and  $L_1=0.132 \mu\text{m}$  into Eq. (1) yields  $E=0.364$  eV (at 110 K). This energy, obtained from nearly the end of the modulation of the QDs, shall correspond to the tail of the EGS. As mentioned above, this energy shall be close to that of the defect state ( $0.37$  eV) because Fig. 5(a) shows that the tail of the QD is immediately followed by the defect state. This consistency supports the validity of using a compensated concentration in a Schottky depletion model to describe the electronic energy band in the bottom GaAs layer near the QDs. Note that we have used this compensated background concentration  $N_D'=2.9 \times 10^{16} \text{ cm}^{-3}$  to obtain the confinement energy of the EGS which is  $E=0.252$  eV. This energy and the PL ground emission ( $1.078$  eV at 110 K) results in the confinement en-

ergy of a HGS of  $1.50 - 1.078 - 0.252 = 0.170$  eV, giving rise to a ratio of the confinement energy of EGS to HGS of 0.60 to 0.40, in agreement with a ratio obtained from the nonrelaxed QDs. Note that this  $N_D' = 2.9 \times 10^{16}$  cm<sup>-3</sup> was also used for the simulation in Fig. 2 to produce a *C* plateau peaked at  $-2.8$  V from an electron state at 0.252 eV.

The EGS at 0.252 eV with its tail at 0.364 eV suggests a tail as wide as 112 meV. A long low-energy tail is also seen in the PL ground emission of the relaxed QDs in Fig. 4, which display a tail extending to about 1300 nm, about 117 meV from the peak of the ground emission at 1.071 eV. Note that this long low-energy tail is not seen in the nonrelaxed QDs, and thus it is related to strain relaxation. Strain relaxation can enhance the fluctuation of the QD states and form a long low-energy tail, suggesting the process is not very homogenous.<sup>19</sup> Note that the carrier compensation effect caused by the relaxation-induced defect state can increase  $L_1$  from 0.074 to 0.132  $\mu\text{m}$  at the tail of the EGS. This, along with the reduction in  $N_D$  from  $8 \times 10^{16}$  to  $2.9 \times 10^{16}$  cm<sup>-3</sup>, would reduce the electric field at the QD from  $8.2 \times 10^6$  to  $5.3 \times 10^6$  V/m from the expression  $E = (q/\epsilon)N_D'L_1$ . As a result, the tunneling emission is significantly suppressed, resulting in a long emission time in the relaxed QDs.

### C. Effect of the free carrier modulation in the top GaAs layer

Probably due to the large  $L_1$ , the free electrons in the top GaAs layer when they traverse through the QD region to the bottom GaAs layer will exert an observable time constant. The *C-V* spectra in Fig. 5(a) display frequency dispersion from 0 to  $-1.5$  V (with a nearly temperature-independent inflexion frequency of about  $6 \times 10^5$  Hz determined from *C-F* spectra). As explained in the section of the theory, this is the modulation of the free electrons in the top GaAs layer with  $C_L = C_2 + C_{\text{GaAs}}$  and  $C_H = C_2$ . The  $C_{\text{GaAs}} = C_L - C_H = 40$  pF at the starting modulation of the QDs (at  $-1.5$  V) gives  $Q_{\text{GaAs}} = 4.8 \times 10^8/\text{cm}^2$  from  $C_{\text{GaAs}} = (1/kT)Q_{\text{GaAs}}$ . This free-carrier modulation effect if not removed would lead to an overestimation of the electron density for the shallow QD electrons. This modulation diminishes rapidly with reverse voltage by  $C_{\text{GaAs}} = C_{\text{GaAs},o} \exp(-V_1/kT)$ . For example, this effect decays to  $e^{-1}$  when the applied voltage probes the QD electrons at  $E = 36$  meV ( $V_1 = 9.5$  meV at 110 K). Thus, it affects only the shallow QD electrons. At around  $-1.5$  V,  $C_1$  can be considered not exist ( $L_1 \rightarrow 0$ ) and  $C_L = C_2 + C_Q + C_{\text{GaAs}}$  and  $C_H = C_2$ . Thus, we remove this free carrier modulation effect by subtracting  $C_L$  from  $C_{\text{GaAs}}$  and the result is shown in the dashed curve in Fig. 6. In this figure, we have converted the reverse voltage to the confinement energy *E* of the QD from the high-frequency capacitance as shown in the inset. From the lowest frequency of 1 kHz which allows the modulation of all the QD electrons, the QD electrons are filled from  $\sim 0.38$  eV to the GaAs CB edge. In the figure, we have marked the EGS and first excited state of the QDs based on the PL spectra. From  $C_L = ((C_1 + C_Q)C_2 / (C_1 + C_Q) + C_2)$  shown in the theory, we obtained  $C_Q$  and estimated the

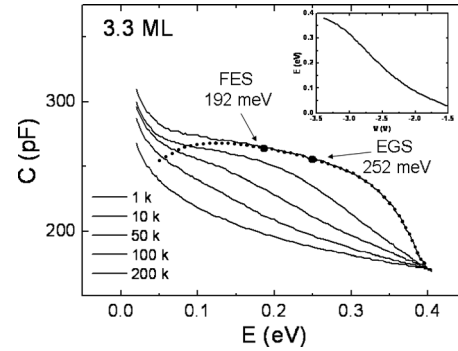


FIG. 6. Measured capacitance vs the confinement energy of the QD electrons converted from Fig. 5(a) using the high-frequency capacitance. The inset shows the converted relationship between reverse voltage and the confinement energy.

total electron density about  $2 \times 10^{11}$  cm<sup>-2</sup>. Thus, each QD contains about eight electrons (QD density  $\sim 3 \times 10^{10}$  cm<sup>-2</sup>).

## IV. CONCLUSIONS

We present a differential capacitance analysis to establish the electronic band structure in strain relaxed InAs QDs. Strain relaxation can introduce a deep defect state to compensate the ionized impurity in the bottom GaAs layer, resulting in a wide depletion width and a long emission time. We show the validity of using a compensated background concentration in a Schottky depletion model to describe the electronic energy band in the GaAs bottom layer. The EGS of the QDs is obtained to be 0.252 eV, giving a ratio of the confinement energies of the electron to HGSs of 0.60 to 0.40. This analysis shows the presence of a long tail for the EGS of the QDs, consistent with the PL spectra.

## ACKNOWLEDGMENTS

The authors are grateful to Dr. J. Y. Chi and R. S. Hsiao for sample preparation and would like to thank the National Science Council of the Republic of China, Taiwan for financially supporting this research under Contract No. NSC-97-2112-M-009-014-MY3. This work is partially supported by MOE ATU program.

<sup>1</sup>F. Heinrichsdorff, M. H. Mao, N. Kirstaedter, A. Krost, and D. Bimberg, *Appl. Phys. Lett.* **71**, 22 (1997).

<sup>2</sup>D. J. Eaglesham and M. Cerullo, *Phys. Rev. Lett.* **64**, 1943 (1990).

<sup>3</sup>D. Leonard, K. Pond, and P. M. Petroff, *Phys. Rev. B* **50**, 11687 (1994).

<sup>4</sup>J. M. Moison, F. Houzay, F. Barthe, and L. Leprince, *Appl. Phys. Lett.* **64**, 196 (1994).

<sup>5</sup>C. W. Snyder, J. F. Mansfield, and B. G. Orr, *Phys. Rev. B* **46**, 9551 (1992).

<sup>6</sup>H. Shoji, K. Mukai, N. Ohtsuka, M. Sugawara, T. Uchida, and H. Ishikawa, *IEEE Photon. Technol. Lett.* **7**, 1385 (1995).

<sup>7</sup>G. Yusa and H. Sakaki, *Electron. Lett.* **32**, 491 (1996).

<sup>8</sup>J. C. Campbell, D. L. Huffaker, H. Deng, and D. G. Deppe, *Electron. Lett.* **33**, 1337 (1997).

<sup>9</sup>C. M. A. Kapteyn, F. Heinrichsdorff, O. Stier, R. Heitz, M. Grundmann, and P. Werner, *Phys. Rev. B* **60**, 14265 (1999).

<sup>10</sup>P. N. Brunkov, A. Patane, A. Levin, L. Eaves, P. C. Main, Y. G. Musikhin, B. V. Volovik, A. E. Zhukov, V. M. Ustinov, and S. G. Konnikov, *Phys. Rev. B* **65**, 085326 (2002).

<sup>11</sup>W. H. Chang, W. Y. Chen, T. M. Hsu, N. T. Yeh, and J. I. Chyi, *Phys. Rev. B* **66**, 195337 (2002).

- <sup>12</sup>X. Letartre, D. Stievenard, and M. Lanoo, *J. Appl. Phys.* **69**, 7336 (1991).
- <sup>13</sup>H. Drexler, D. Leonard, W. Hansen, J. P. Kotthaus, and P. M. Petroff, *Phys. Rev. Lett.* **73**, 2252 (1994).
- <sup>14</sup>S. Sauvage, P. Boucaud, F. H. Julien, J.-M. Gerard, and J.-Y. Marzin, *J. Appl. Phys.* **82**, 3396 (1997).
- <sup>15</sup>H. L. Wang, F. H. Yang, S. L. Feng, H. J. Zhu, D. Ning, H. Wang, and X. D. Wang, *Phys. Rev.* **61**, 5530 (2000).
- <sup>16</sup>J. Ibáñez, R. Leon, D. T. Vu, S. Chaparro, S. R. Johnson, C. Navarro, and Y. H. Zhang, *Appl. Phys. Lett.* **79**, 2013 (2001).
- <sup>17</sup>J. F. Chen, R. S. Hsiao, C. K. Wang, J. S. Wang, and J. Y. Chi, *J. Appl. Phys.* **98**, 013716 (2005).
- <sup>18</sup>J. F. Chen, Y. Z. Wang, C. H. Chiang, R. S. Hsiao, Y. H. Wu, L. Chang, J. S. Wang, T. W. Chi, and J. Y. Chi, *Nanotechnology* **18**, 355401 (2007).
- <sup>19</sup>J. F. Chen and J. S. Wang, *J. Appl. Phys.* **102**, 043705 (2007).
- <sup>20</sup>J. F. Chen, N. C. Chen, J. S. Wang, and Y. F. Chen, *IEEE Trans. Electron Devices* **48**, 204 (2001).
- <sup>21</sup>J. F. Chen, R. S. Hsiao, Y. P. Chen, J. S. Wang, and J. Y. Chi, *Appl. Phys. Lett.* **87**, 141911 (2005).
- <sup>22</sup>S. D. Lin, V. V. Ilchenko, V. V. Marin, K. Y. Panarian, A. A. Buyanin, and O. V. Tretyak, *Appl. Phys. Lett.* **93**, 103103 (2008).
- <sup>23</sup>Y. Uchida, H. Kakibayashi, and S. Goto, *J. Appl. Phys.* **74**, 6720 (1993).